Journal of Stress Analysis
Vol. 6, No. 1, Spring − Summer 2021, 105-125

Bu-Ali Sina University

ORIGINAL RESEARCH PAPER

Effect of Process Parameters on Thin-wall Products under High-frequency Vibrating Tools, Case Study: Ultrasonic Assisted Deep Drawing Process

A.A. Naderi[a,*], **S.A. Mokhtari**[b]
[a]Department of Mechanical Engineering, Imam Ali University, Tehran, Iran.
[b]Department of Flight and Engineering, Imam Ali University, Tehran, Iran.

Article info

Article history:
Received 14 June 2021
Received in revised form
08 September 2021
Accepted 11 September 2021

Keywords:
Ultrasonic vibration
Deep drawing
Thin metallic sheets
Finite element simulation
Parametric study

Abstract

Ultrasonic Assisted Deep Drawing (UADD) is a state of the art Conventional Deep Drawing (CDD) process that results in improved formability and decrease in forming force. In this novel technology, the forming tool fluctuates under low amplitude and high frequency which is supplied by an ultrasonic package including generator and transducer. The main objective of this research is study of various parameters affecting the deformation behavior of the formed thin cylindrical-parts by UADD process, based on experimental tests and numerical methods followed by statistical approach. In this regard, a sophisticated Finite Element Model (FEM) including surface effect and stress superposition is developed. Nevertheless, a robust technological equipment is designed and fabricated in which the special die as a main vibratory tool can be longitudinally stimulated by enforced vibrations with frequency very close to the 20kHz. Consequently, experiments are performed to determine the effectiveness of the ultrasonic vibration, as well as, calibrate the established FE model. The simulation outputs and the relevant experimental tests are compared based on the forming force and drawing depth results, and an acceptable agreement is achieved. Based on the validated numerical model, Design of Experiment (DOE) by Response Surface Methodology (RSM) is utilized to run multiple simulations. Moreover, the effect of six parameters in the UADD process on the maximum forming force and the minimum thickness of the formed cup is statistically evaluated and high-reliability regression models based on the analysis of variance (ANOVA) with 90 simulations are generated to estimate these two output parameters. As a result, ultrasonic vibration amplitude, punch nose radius, and blank diameter with 37.22, 21.68, and 19.03% of contribution, respectively, were the most effective parameters on the required forming load. Furthermore, the results illustrated that ultrasonic vibration amplitude was the most important parameter on thickness reduction of sheet with 69.92% contribution.

Nomenclature

ANOVA	Analysis of variance	STH	Shell thickness (mm)
r_0	Anisotropic parameter 0	K	Strength coefficient (MPa)
r_{45}	Anisotropic parameter 45	n	Strain hardening exponent

*Corresponding author: A.A. Naderi (Assistant Professor)
E-mail address: aa.naderi@modares.ac.ir
http://dx.doi.org/10.22084/jrstan.2021.24744.1187
ISSN: 2588-2597

r_{90}	Anisotropic parameter 90	Y_s	Tensile strength (MPa)
w	Angular frequency (rads^{-1})	t	Time (s)
CDD	Conventional deep drawing	t_f	Thickness of the final cup wall (mm)
$\bar{\sigma}$	Effective stress (MPa)	ε_t	Thickness strain
e_0	Engineering strain	UADD	Ultrasonic assisted deep drawing
$\bar{\varepsilon}$	Equivalent strain	$A_{\max}$	Vibration amplitude (μm)
FLD_0	Forming limit diagram	f	Vibration frequency (s^{-1}, Hz)
t_0	Initial thickness (mm)	Y_0	Yield strength (MPa)
e_θ	Main engineering strain	E	Young modulus (MPa)
RSM	Response surface method		

1. Introduction

Deep drawing is extensively used as a common method in sheet metal forming process having a variety of industrial applications such as aviation equipment, automotive, and home appliances. The tendency of controlling the governing parameters in the sheet metal forming process is due to the occurred defects like variation of the sheet thickness and rupture that makes the process complicated and affects the quality of products. As shown schematically in Fig. 1, a thin blank is subjected to plastic deformation using forming tools (punch) to give the blank a desired shape by controlling the blank-holder that prevents wrinkling during the forming operation. The aim is to achieve thin drawn parts with higher depth while the formability of the sheet increases.

For this purpose, various methods including hydroforming [1], warm forming [2], using electromagnetic pulse [3], flexible tools [4], low-frequency oscillatory blank-holder [5] and punch with micro-ridges [6] has been outlined by many scientists. Nowadays, ultrasonic forming as booming research with superior merits such as decreasing forming load as well as friction force, and increasing formability [7] has been attracting the attention of many researchers. Research has documented that the application of Ultrasonic Vibrations (UV) during the metal plasticity results in the absorption of ultrasonic energy locally at the imperfections of material crystalline lattices such as vacancies, dislocations, and grain boundaries, implicitly; the interatomic agitation caused by UV favors the formability of material [8].

In 1955, Blaha and Langencker [9] were pioneers in studying the deformation behavior and microstructural change on zinc single crystal during ultrasonic-assisted tension test experimentally. In this study, a series of uniaxial tensile tests on the Zn single crystal was performed under ultrasonic waves ranging from 50 to 80kHz. They found that the material flow stress was markedly reduced in UV condition compared with the static tensile test, the phenomenon which was later investigated as Blaha effect, acoustic softening, and volume effect [10]. Moreover, the use of UV energy changes interfaces friction between the tool and workpiece and leads to reduce the friction force, which the advantage ascertained as a surface effect [11]. Continuous research in this area revealed that utilization of vibratory tool in forming processes would increase the plastic strain of material. This result has been attributed to the static and dynamic load superposition [12]. Despite the aforementioned benefits of UV application and its disclosure in bulk metal forming processes, especially Equal Channel Angular Pressing (ECAP) [13] and upsetting [14], few efforts have been directed at utilizing this technique to improve drawability of sheet metal in forming processes.

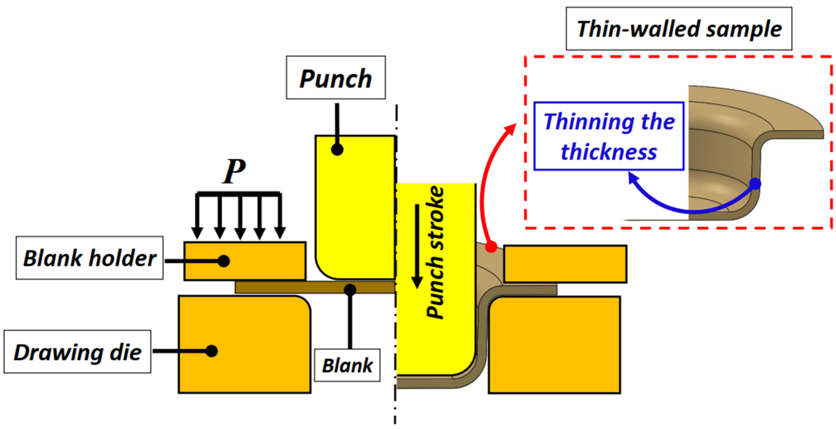

Fig. 1. Schematic concept of conventional deep drawing process.

Vahdati et al. [15] applied ultrasonic-assisted incremental forming to improve surface roughness and spring-back of the formed sheet. In further work, Amini et al. [16] investigated UV application in incremental forming to enhance the formability of annealed AL1050 sheets. Based on their results UV application with 7.5μm amplitude and 20,000Hz frequency will lead to an increase in plastic strain up to 48%. Long et al. [17] studied the influence of ultrasonic-assisted incremental forming process parameters namely sheet materials, amplitude vibration, tool diameter, and feeding speed by a series of experimental tests and multiple finite element simulations. The results of the experimental tests showed that UV energy significantly leads to an increase in the temperature of the formed sheet. They illustrated that increased temperature helps to be formed, and leads to the release of residual stresses. The results of the simulation showed that with increasing the amplitude of ultrasonic vibrations, the plastic strain in the contact area between the tool and the work-piece increases. Pengyang Li et al. [18] developed a 3D finite element model in ABAQUS software to evaluate the various components of the forming force in UV-assisted incremental forming. Numerical results showed that the axial component of the force in the oscillatory tool decreases continuously with increasing amplitude of ultrasonic vibrations. Their analysis of different frequencies revealed that by selecting values above 40kHz for the vibrational frequency, a phenomenon called rebound occurs for the oscillatory tool, which leads to an increase in the forming force. Pasierb and Wonjar [19] experimentally applied ultrasonic vibrations (16kHz) to the drawing die by magnetostrictive transducers. The results of their experimental tests showed that using ultrasonic oscillations leads not only to reduction of the forming force but also the uniform thickness variation in the wall of the work-piece. Jimma et al. [20] experimentally investigated the ultrasonic-assisted deep drawing process. They applied UV individually and in combination with each of the punch, die and blank holder. Their results showed that ultrasonic vibrations can increase the drawing depth of blank. They showed that the application of ultrasonic vibrations to the die resulted in a 10% increase in Limiting Drawing Ratio (LDR), while simultaneous vibration of the blank holder and die can increase this ratio up to 14%.

According to the experimental studies, the contribution of surface effect shows a more dominant role in improving the forming process than that of acoustic softening [21]. Therefore, finite element modeling of ultrasonic forming processes, regardless of the volume effect, can provide an acceptable prediction [13]. Hence, a three-dimensional model of the ultrasonic-assisted press forming process was proposed by Ashida and Ayoma [22]. By using multiple simulations, they indicated that ultrasonic vibrations (21kHz) have a significant effect on the reduction of the friction factor between the edge radius of the die and the work-piece. This reduction of friction also prevents the rupture of the sample into the edge radius of the die in addition to the reduced forming force. Malekipour et al. [23] studied the ultrasonic deep drawing process experimentally and numerically. By analyzing a vibrational model and excitation frequency, they investigated the effect of resonant frequency variation on the forming limit, the forming force, the frictional force and the material flow stress qualitatively. They declined that reducing the frictional force is a consequence of increasing the internal energy of the blank in the plastic deformation zone; meanwhile, Interatomic agitation favors the sliding of the crystallographic planes into the structural network of the blank.

Due to the complexity of different parameters' combination in the UADD, finding the most effective parameters in the process is vital. The aim of this study is to investigate the effect of different parameters in the UADD. Aside from the conventional deep drawing parameters, the UV parameters such as vibration amplitude and frequency can significantly affect the forming process results. However, since the experimental tests at different vibrational frequencies are time-consuming and costly, finite element simulation is employed as a powerful tool to reduce design and experiment costs. Several different factors have impact on ultrasonic-assisted deep drawing process. Simulating and analyzing of these factors is a time and power consuming process. In order to have more efficient approach in the study, the design of experiment is the best choice to reduce the number of simulations with having the same acceptable results.

In the present study, the effect of ultrasonic deep drawing parameters on the forming force and thickness reduction is investigated. For this purpose, a customized ultrasonic die was designed and manufactured precisely to vibrate at 20kHz frequency in the axial direction with the longitudinal mode shape under resonance conditions. Then, in the second phase, the experimental tests and simulations were performed under conventional and vibrational conditions with 5μm vibration amplitude. In the third phase, by using Response Surface Methodology (RSM) the effect of process parameters on deformation behavior was investigated.

2. Materials and Methods

In this section, a brief description of the design parameters and specifications, material and their properties and experiment condition are provided.

2.1. Material and Uniaxial Tensile Test

In this research, low carbon steel (St12) sheet with a 0.5mm thickness was used. To perform uniaxial tensile test according to ASTM-E8 standard, the dog-bone shaped specimens in the rolling, diagonal, and transverse direction were cut using laser. The specimens through the jaws (grippers) were mounted on the SANTAM universal testing machine. It is worth mentioning that an extensometer was used to measure the strain of the specimen during the uniaxial tensile test. The extensometer was linked to the SANTAM universal tensile device software and could calculate Young's module value in the elastic region. The engineering and true stress-strain diagrams extracted from the tensile test for rolling direction are depicted in Fig. 2. Eq. (1) representing the Holloman hardening power formula based on experimental results. As shown in Fig. 2, R^2 is greater than 0.95 for the fitted curve.

$$\bar{\sigma} = 615.59(\bar{\varepsilon})^{0.312}(\text{MPa}) \tag{1}$$

where $\bar{\sigma}$ and $\bar{\varepsilon}$ are equivalent stress and plastic strain respectively. The mechanical properties of low carbon steel (St 12) sheet in rolling direction are presented in Table 1.

2.2. Ultrasonic Device, UADD Setup and Test Procedure

In order to apply ultrasonic vibration to the forming tool (die), an ultrasonic set including power supply, a piezoelectric transducer, and a booster were connected to the deep drawing die. To provide ultrasound energy, a 3kW power supply, with a wide range of working frequencies, 15,000 to 20,000Hz, was implemented. This generator is capable of scanning and regulating the resonance frequency of the vibratory system. The high-frequency electrical power is sent to the piezoelectric transducer. The transducer consists of the piezoelectric stacks, backing, and matching which are assembled with a pre-stress center bolt. This transducer has a longitudinal natural frequency of 20kHz and a nominal power of 2kW. Booster plays a key role in transferring the ultrasonic wave and improving the output vibration amplitude of transducer. In this study, 316 non-magnetic stainless steel was used for the deep drawing die. For achieving the resonance pulsation, ABAQUS/Frequency was used through the numerical modal analysis. Therefore, to find the resonance frequency of the die, multiple numerical modal analysis was simulated. The results show that the natural frequency of the die in longitudinal mode is 20,064Hz (shown in Fig. 3). It is noteworthy to mention that the calculated value is very close to the natural frequencies of booster and transducer, which satisfies the requirements of the resonant state. Then, based on the final geometry dimensions obtained from the simulated modal analysis, the ultrasonic drawing die was fabricated. The geometrical dimensions of the die are provided in Table 2.

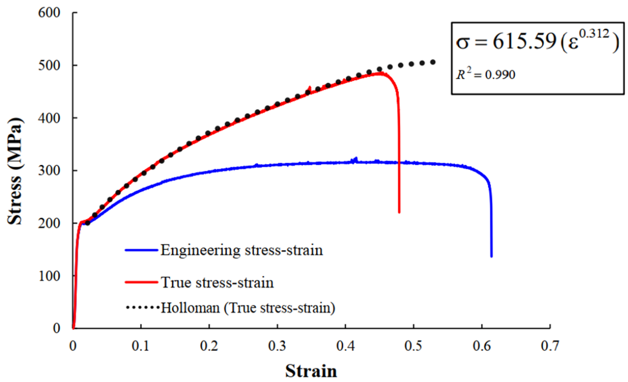

Fig. 2. Strain-stress curves obtained from uniaxial tensile test: engineering diagram, true diagram, and the fitted stress-strain curve in plastic region.

Table 1
Mechanical properties and anisotropy coefficients of low carbon steel (St12) sheet metal.

Properties	Value
Thickness, t_0 (mm)	0.5
Young modulus, E (MPa)	210,000
Yield strength, Y_0 (MPa)	198.944
Tensile strength, Y_s (MPa)	314.896
Strain hardening exponent, n	0.312
Strength coefficient, K (MPa)	615.59
Lankford anisotropy coefficients	
r_0	0.93
r_{45}	1.12
r_{90}	1.34

* r_0, r_{45}, and r_{90} are the r-values along Rolling Direction (RD), Diagonal Direction (DD), and Transverse Direction (TD), respectively

* Holloman law: $\bar{\sigma} = k(\bar{\varepsilon})^n$

Table 2
The geometric dimensions of die.

Parameter	Value (mm)
Punch diameter	17.0
Punch nose radius	4.0
Die cavity diameter	20.0
Die entrance radius	4.0

Fig. 4 shows the details of different parts, assembly and tuning the resonant frequency. The main vibratory set (transducer, booster, and drawing die) as the core of the technological equipment was assembled using double-screw bolts and then, from the flanged portion of the drawing die was fastened to the upper base. In order to prevent the transfer of ultrasonic vibration to the structure of the technological equipment and to reduce the waste of ultrasonic energy, the flanged portion of drawing die as a nodal plane with zero displacement was acoustically isolated. Pillar-shaped spacers fixed blank-holder on the die. Therefore, a 0.6mm fixed gap was between the blank holder and the working surface of the die. Later, the punch with axial constraint against the die cavity was fastened on the lower base.

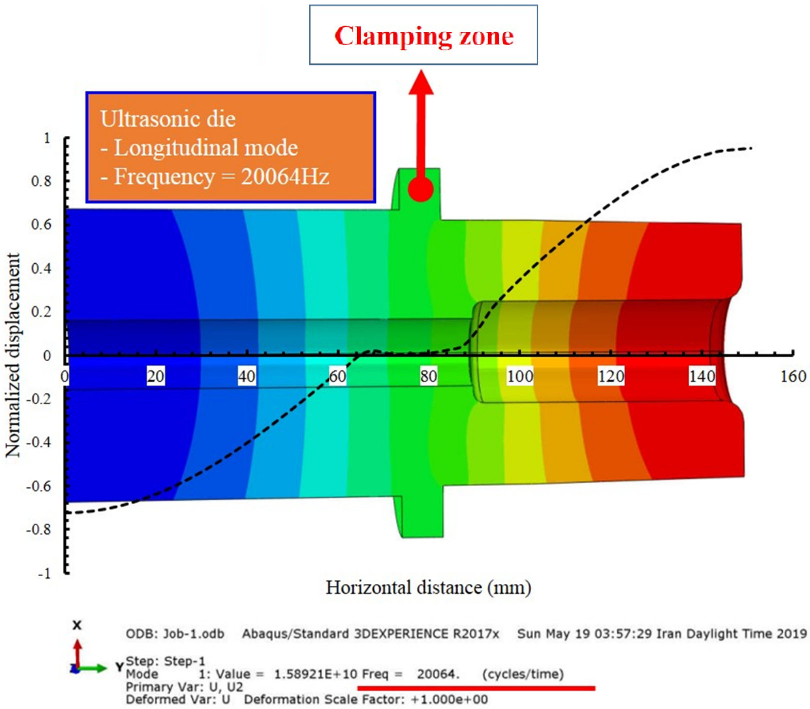

Fig. 3. Simulated modal analysis result for the drawing die (ABAQUS 2017 - longitudinal mode with natural frequency 20064Hz).

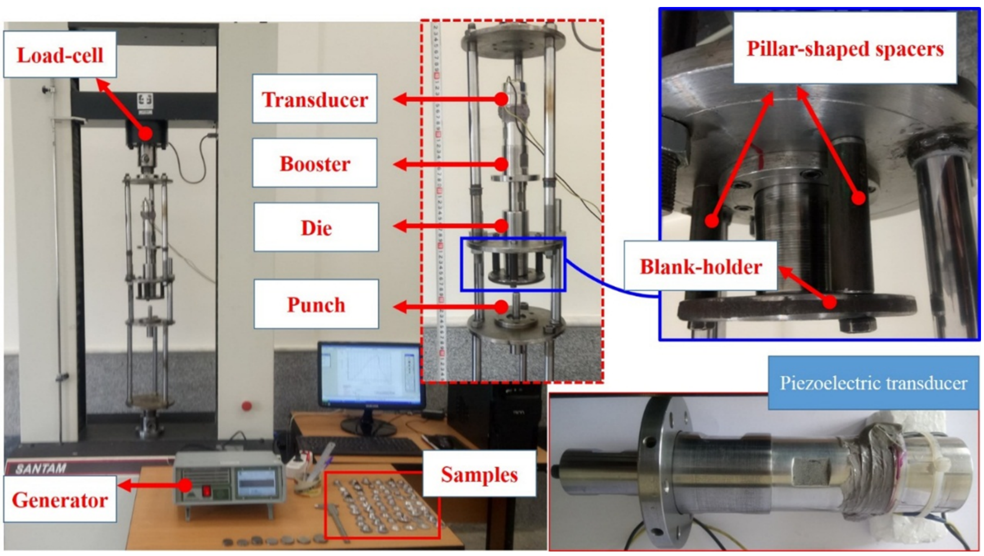

Fig. 4. Technological equipment of ultrasonically assisted deep drawing process: parts, assembly and tuning the resonant frequency.

In this study, experiments were carried out using a computer controlled universal testing machine (Fig. 4). In order to determine the experimental resonant frequency, the die was assembled with a booster and transducer. Then plugged into the technological equipment and tested by the ultrasound generator. After applying the transducer vibrations, the 20,016Hz resonant frequency was obtained under experimental and no-load conditions, which correlated well with the results obtained from the modal analysis (shown in Fig. 5). To measure the static and average forces, respectively, under conventional and ultrasonic vibration conditions, a load-cell was installed on the device. The stroke value of the process was also extracted through the device encoder. For conventional and ultrasonic-assisted deep drawing tests, the blanks with 34mm and 39mm diameter were detached from sheet metal by laser cutting. The tests were performed at a constant speed of 10mm/min at room temperature. It should be noted that in this study no lubricants were used on the surfaces of the die components. Before performing the main tests, the vibration amplitude at the die tip needed to be determined. So, an accurate GAP-Sensor with the model number of PU-05, which is a type of proximity sensor with 0.3μm resolution, was used to measure the vibration amplitude. Moreover, AEC-5505 converter was applied to convert tool tip displacements into electrical signals.

2.3. Description of the Finite Element Model

In this study, ABAQUS/Explicit was used. This commercial finite element code is capable of analyzing sophisticated forming processes. All parts, including die, sheet metal, punch, and blank holder were modeled in a 1:1 scale. Due to axisymmetric design of the die set and to reduce computation cost, only a quarter of die set was analyzed (shown in Fig. 5). The blank part with shell shape was set deformable and the other parts including punch, die and blank holder were considered rigid.

The mechanical properties and stress-strain curve of material are based on Section 2.1. In the modeling, the Hill-48 yield criterion was used as Eq. (2) [24].

$$f(\sigma) = \sqrt{F(\sigma_{22}-\sigma_{33})^2 + G(\sigma_{33}-\sigma_{11})^2 + H(\sigma_{11}-\sigma_{22})^2 + 2L\sigma_{23}^2 + 2M\sigma_{13}^2 + 2N\sigma_{12}^2} \quad (2)$$

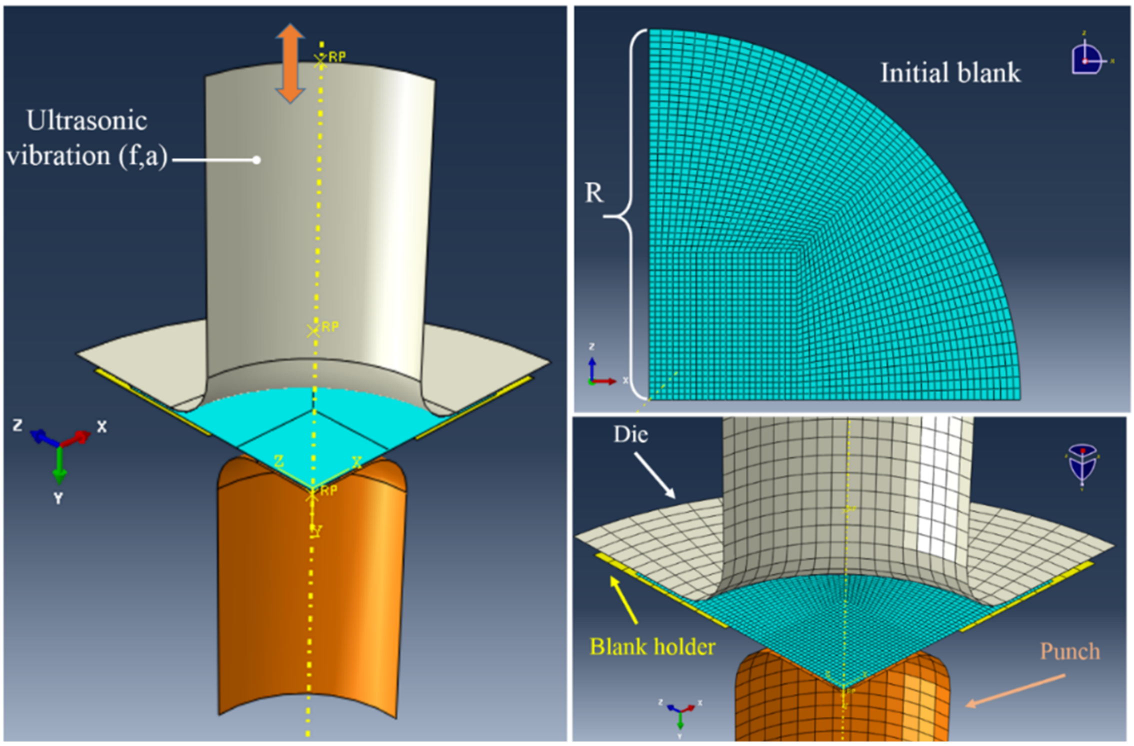

Fig. 5. Finite element model geometry of the ultrasonic assisted deep drawing process (ABAQUS 2017).

F, G, H, L, M, N are the constants of the Hill yields criterion obtained by the Eqs. (3) to (7) [24].

$$F = \frac{1}{2}\left(\frac{1}{R_{22}^2} + \frac{1}{R_{33}^2} - \frac{1}{R_{11}^2}\right) \tag{3}$$

$$G = \frac{1}{2}\left(\frac{1}{R_{33}^2} + \frac{1}{R_{11}^2} - \frac{1}{R_{22}^2}\right) \tag{4}$$

$$H = \frac{1}{2}\left(\frac{1}{R_{11}^2} + \frac{1}{R_{22}^2} - \frac{1}{R_{33}^2}\right) \tag{5}$$

$$L = \frac{3}{2R_{23}^2} \tag{6}$$

$$M = \frac{3}{2R_{13}^2} \tag{7}$$

$$N = \frac{3}{2R_{12}^2} \tag{8}$$

To apply mentioned relations in ABAQUS, the anisotropy coefficients are as Eqs. (8) to (11) [24].

$$R_{11} = R_{13} = R_{23} = 1 \tag{9}$$

$$R_{12} = \sqrt{\frac{3(r_0+1)r_{90}}{(2r_{45}+1)(r_0+r_{90})}} \tag{10}$$

$$R_{22} = \sqrt{\frac{r_{90}(r_0+1)}{r_0(r_{90}+1)}} \tag{11}$$

$$R_{33} = \sqrt{\frac{r_{90}(r_0+1)}{r_0+r_{90}}} \tag{12}$$

It is generally accepted that the advantages of ultrasonic waves in metal forming are a combination of the acoustic softening phenomenon and the surface effect [25], so in order to take into account the acoustic softening, the uniaxial tensile test with superimposing UV was performed. As shown in Fig. 6a, a special setup was designed and constructed to extract softened material data in different vibrational amplitudes. The set is designed in such a way that the specimen can oscillate longitudinally. The result of modal analysis shows that the highest amplitude of vibration takes place in the gauge length. The stress vs strain curve in three different amplitudes is presented in Fig. 6b. It is clear that due to the acoustic softening phenomenon induced by ultrasonic energy, the material flow stress decreases with increasing vibration amplitude. Hence, for simulation in each vibrational amplitude, the behavior of the respective softened material is included.

Punch, die and blank holder were modeled using shell elements with type node 3-D bilinear rigid quadrilateral (R3D4), while the blank meshed with 4-node shell elements (S4R). The mesh size evaluation was performed regarding the amount of kinetic energy dived to internal energy. The size was accurate when this ratio approached the least amount and can be ignored. In order to apply ultrasonic vibrations to the simulation, a low-amplitude and high-frequency displacement were added to the static motion of the die corresponding to Eqs. (12) and (13) [26]. Hence, a VDISP* subroutine was developed in FORTRAN compiler and implemented in ABAQUS.

$$u = \nu(t) + A_{\max}\sin(wt) \tag{13}$$

$$w = 2\pi f \tag{14}$$

where $A_{\max}$, w, and t represent the maximum vibration amplitude, angular frequency, and time parameter, respectively. The constraint type between punch and blank, blank and blank holder, and blank with die was surface-to-surface contact. Thus, Coulomb friction model and penalty method were adopted between the interfaces of the tool. Table 3 provides the interface coefficient of friction considered in this simulation. The friction coefficient of 0.15 and 0.25 reflects the dry friction conditions, which is similar to the experimental values in this study [5].

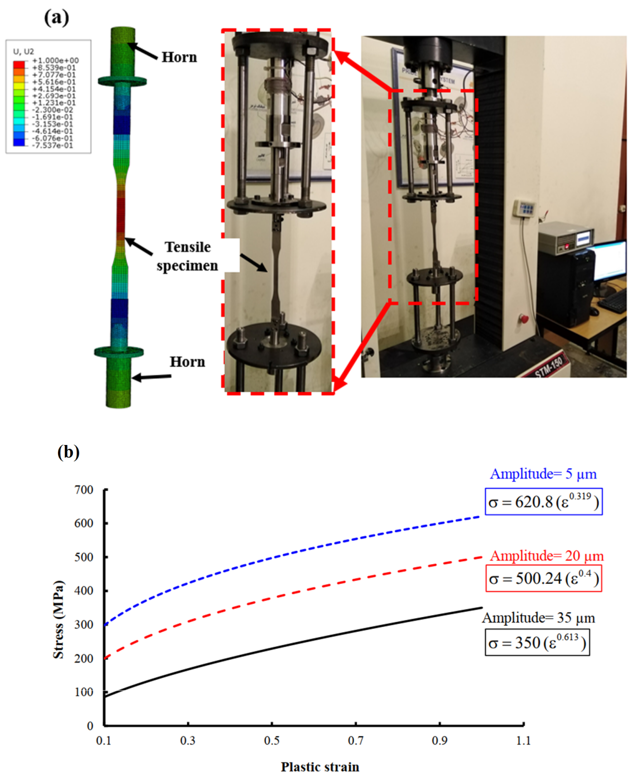

Fig. 6. Ultrasonic assisted uniaxial tension test: a) Design, construction and experimental setup, b) Power formula fitted for stress vs strain curve in three different amplitudes.

Table 3
Coefficient of friction between surfaces in simulation [5].

Interfaces	Friction coefficient
Punch/blank	0.15
Blank holder/blank	0.15
Die/blank	0.25

2.4. Failure Criterion

As the failure criterion, the maximum thinning (t_f), was checked. The maximum thinning was calculated by the thick strain ε_t from forming limit diagram (FLD_0), Eq. (14). Where t_0 is the initial thickness of the blank and t_f is the thickness of the final cup wall. The principal engineering strain e_0 in the plane-strain condition was obtained based on the empirical equation provided by the North American Deep Drawing Research Group [27]. It is estimated as shown in Eq. (15):

$$t_f = t_0 e^{(\varepsilon_t)} \tag{15}$$

$$e_\theta = FLD_0 = \left(23.3 + \frac{360}{25.4}t_0\right)\left(\frac{n}{0.21}\right) \tag{16}$$

That FLD_0 is the main engineering strain under the plane-strain condition, n is the strain hardening exponent, e_θ is the main engineering strain, and t_0 is the initial sheet thickness. Engineering strain in plane-strain condition can be written as the true strain by Eq. (16). Assuming constant volume, Eq.(17), and $\varepsilon_z = 0$ (plate strain condition), the true strain in the thickness direction is determined by Eq. (18) [27]:

$$\varepsilon_\theta = \ln(1 + e_\theta) \tag{17}$$

$$\varepsilon_\theta + \varepsilon_z + \varepsilon_t = 0 \tag{18}$$

$$\varepsilon_t = -\varepsilon_\theta \tag{19}$$

Finally, with respect to $n = 0.321$, the fracture thickness is 0.304mm, which is the most thinning value.

3. Results and Discussion

In this section, the results of experimental tests related to the reduction of the drawing force and the increase of the draw-ability with the frequency of 20kHz and 5μm amplitude of ultrasonic vibrations are presented.

3.1. Experimental Results

Fig. 7 shows the formed cups in both conventional and ultrasonic vibrational conditions. Initially, blanks with 34mm initial diameter were fully formed under conventional conditions without rupture. Therefore, this size of the initial blank diameter could not disclose the UV energy effect on the increase in formability. Hence, the size of the initial blank diameter increased. Subsequently, a conventional deep drawing operation for blanks with an initial diameter of 39mm was performed, and as shown in Fig. 7, the formed work-piece broke at 8mm depth. Therefore, metal blanks with an initial diameter of 39mm were used for deep drawing tests with ultrasonic vibration. High-frequency vibrations were applied continuously from the beginning to the end of the deep drawing process, and the cup was completely deformed without any cracks and no tearing, resulting in a 12.2% increase in the drawing ratio.

Fig. 8 shows the average forming force related to 39mm blank. As can be seen, due to the tuned out condition of the system, the forming process with ultrasonic shows no decrease in forming force at the beginning. When the force decreases, the maximum amount of forming force decreases by 6% for continuous vibrational conditions.

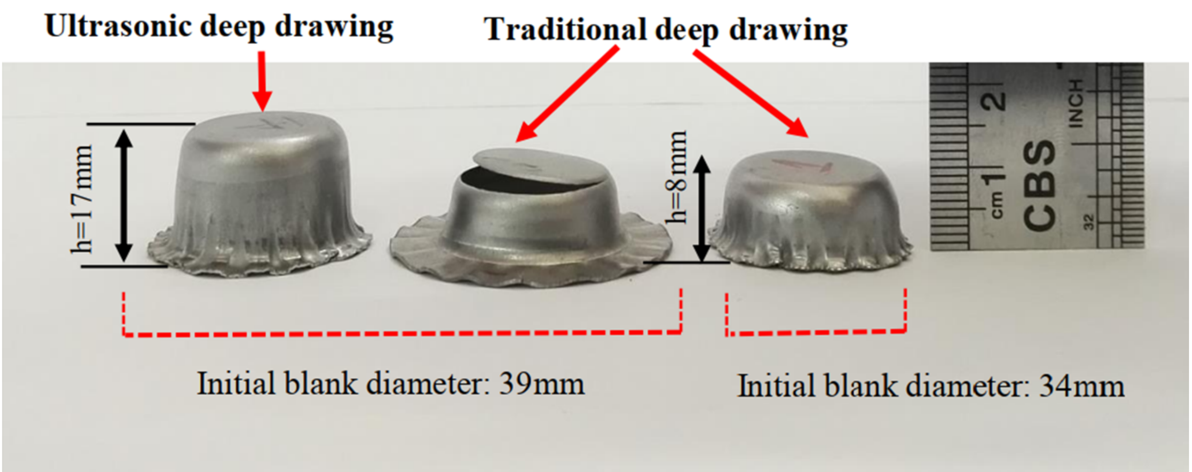

Fig. 7. Increased sheet formability in the presence of ultrasonic vibrations for blanks with an initial diameter of 39mm and vibration frequency of 20kHz and 5μm amplitude.

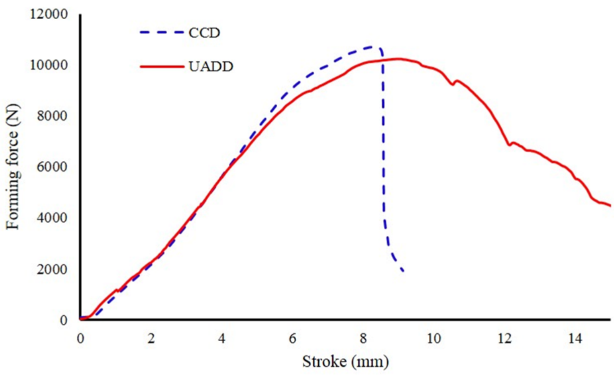

Fig. 8. Forming force in conventional and ultrasonic deep drawing (frequency 20kHz, amplitude 5μm).

In order to validate the finite element model, the results of simulations for blanks with an initial diameter of 39mm under conventional and UV conditions (20kHz and 5μm amplitude) were compared to the experimental results. The validation of the FEM was based on the formed cups configuration and forming force results. Fig. 9, 10, and 11 provide the configurations and forming forces for deep drawn cups, numerically, and experimentally. The thickness distribution contour (STH) of the CDD and UADD processes is shown in Figs. 9 and 10. During conventional deep drawing, the blank was ruptured with 8mm depth, while the corresponding numerical simulation results showed a rupture at 9.63mm depth (Fig. 9). Accordingly, there is a 17% difference between the simulation and experimental test results which can be attributed to the measurement method accuracy and neglecting the wrinkling area of the sample flange. The results of deep-drawn cups with ultrasonic vibrations are shown in Fig. 10. In this case, the minimum thickness is greater than the minimum permissible of 0.321mm, which approved the finite element simulations prediction. Moreover, the blanks are completely deformed without any rupture. The obtained forming force of finite element simulation and the experimental results are compared in Fig. 11a and 11b. Based on these plots, the overall forming force prediction from the FE simulation and experiments have same trends.

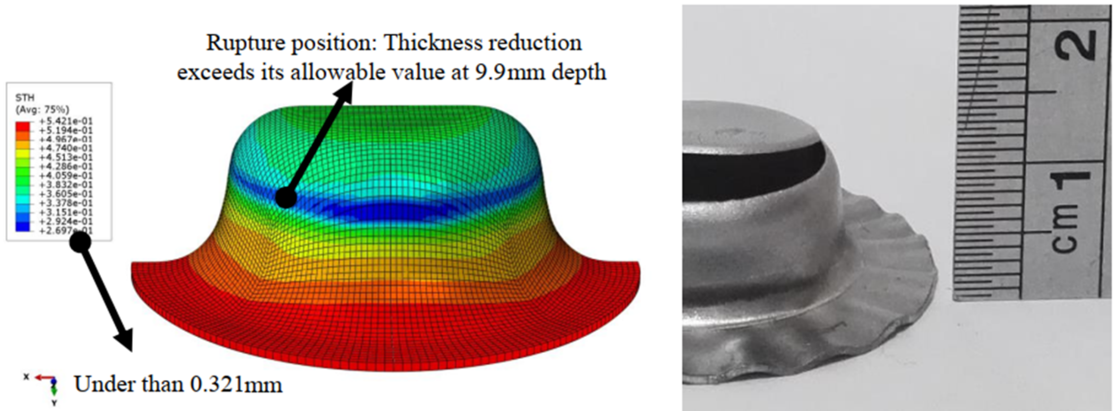

Fig. 9. Comparison between formed cups with simulation and experimental approach under conventional deep drawing (CDD) condition.

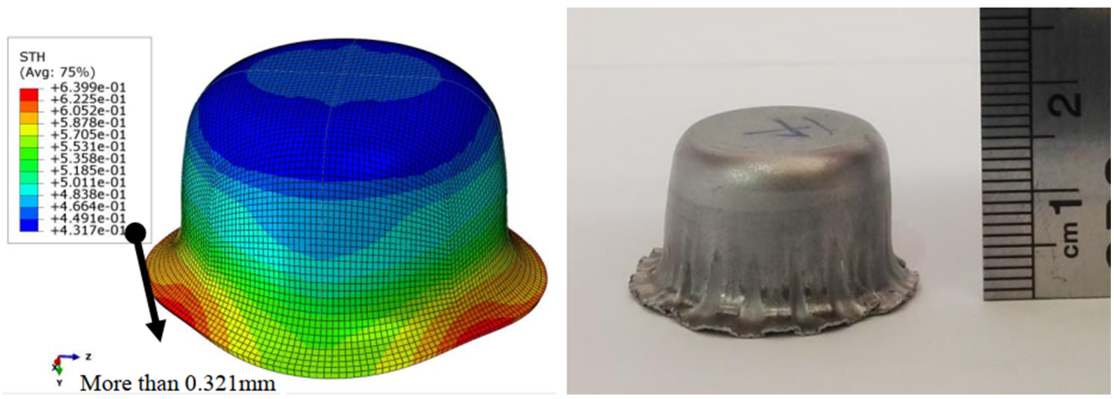

Fig. 10. Comparison of the formed cup of the experimental work with finite element simulations, ultrasonic deep drawing (20kHz vibration frequency and 5μm vibration amplitude).

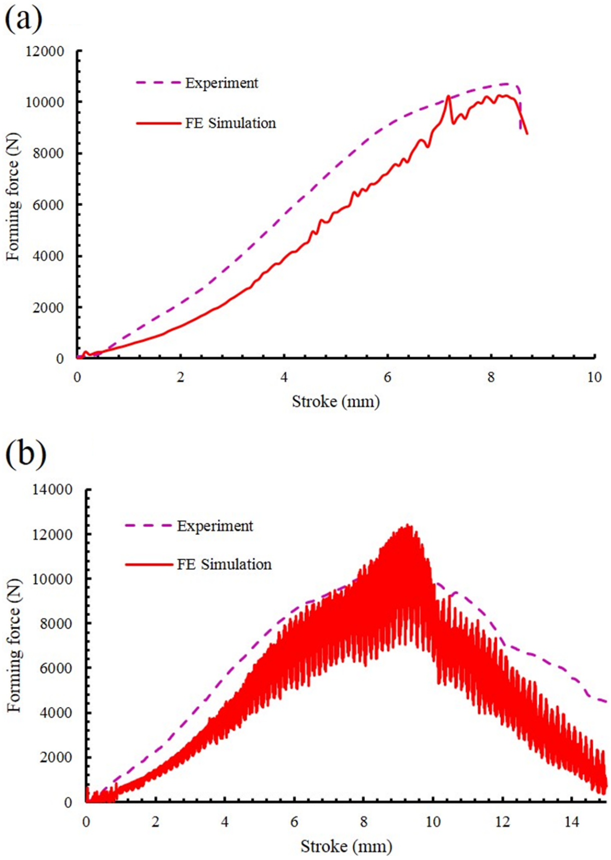

Fig. 11. Comparison between the forming forces obtained in experimental work with finite element simulation. a) Conventional deep drawing, b) Ultrasonic deep drawing (20kHz frequency and 5μm vibration amplitude).

Fig. 11b shows the forming force during the UADD process for the formed cup. The load cell shows an average decrease in the forming force due to the presence of ultrasonic vibrations. However, the load cell was not capable of measuring the oscillatory force. The FE simulation implementation can accurately exhibit the oscillatory forces caused by the presence of ultrasonic. Table 4 shows the numerical and experimental forming force values for CDD and UADD. The results show 6% and 8% force reduction in the experimental and simulated ultrasonic-assisted deep drawing, respectively.

3.2. Simulation Results on the Deformation Behavior of Thin-wall Products

Fig. 12 shows the thickness distribution contour (STH) in constant vibration amplitude of 5μm with different frequencies. As can be seen from this figure, the minimum thickness is located in the circumference of the cup bottom. The best thickness distribution is obtained for a vibration frequency of 35kHz. Fig. 12c contours show that by increasing the frequency beyond 35kHz the thinning increase due to the rebounding in the ultrasonic process. The rebound decreases the separation time of die and blank. Thus, increasing the frequency in the range beyond 35kHz, despite the increase in force, thinning also occurs for the formed cup.

Fig. 13 illustrates the effect of the vibration amplitude on the thickness distribution of the drawn parts. Hence, at a constant frequency of 20kHz, the simulations were performed in four cases of different vibrational amplitudes. The results indicate the application of a 10μm vibration amplitude compared to other conditions provided the optimum thickness distribution. However, increasing the vibration amplitude above this value increases the thinning in the radius of the bottom cup. This process continues until the vibrational amplitude of 35μm (shown in Fig. 13d) causes the greatest thinning in the radius of the cup bottom. This value is close to the maximum thinning of sheet thickness (0.321mm). Therefore, increasing the vibration amplitude, although significantly reduces the forming force, causes a severe decrease in the formed cups, and this is not beneficial to the process, hence the choice of optimum vibration amplitude and frequency improves the process. The parametric study of the process is also presented in the next section to further investigate the effect of vibration amplitude and frequency.

3.3. Numerical Study Procedure

In this study, to reduce the costs and time of the experiments, Response Surface Method (RSM) was implemented. RSM is one of the powerful mathematical and statistical methods to predict process outputs (response variables) by considering independent design parameters (input variables).

Table 4
Comparison of experimental and simulation results of maximum average forming force for conventional and ultrasonically assisted deep drawing process.

Process	Maximum average force (kN)		Error (%)
	Experiment	FE simulation	
Conventional deep drawing (CDD)	10.7	10.22	4.5
Ultrasonically assisted deep drawing (UADD)	9.8	9.43	6.6
Force reduction (%)	8.4	8	

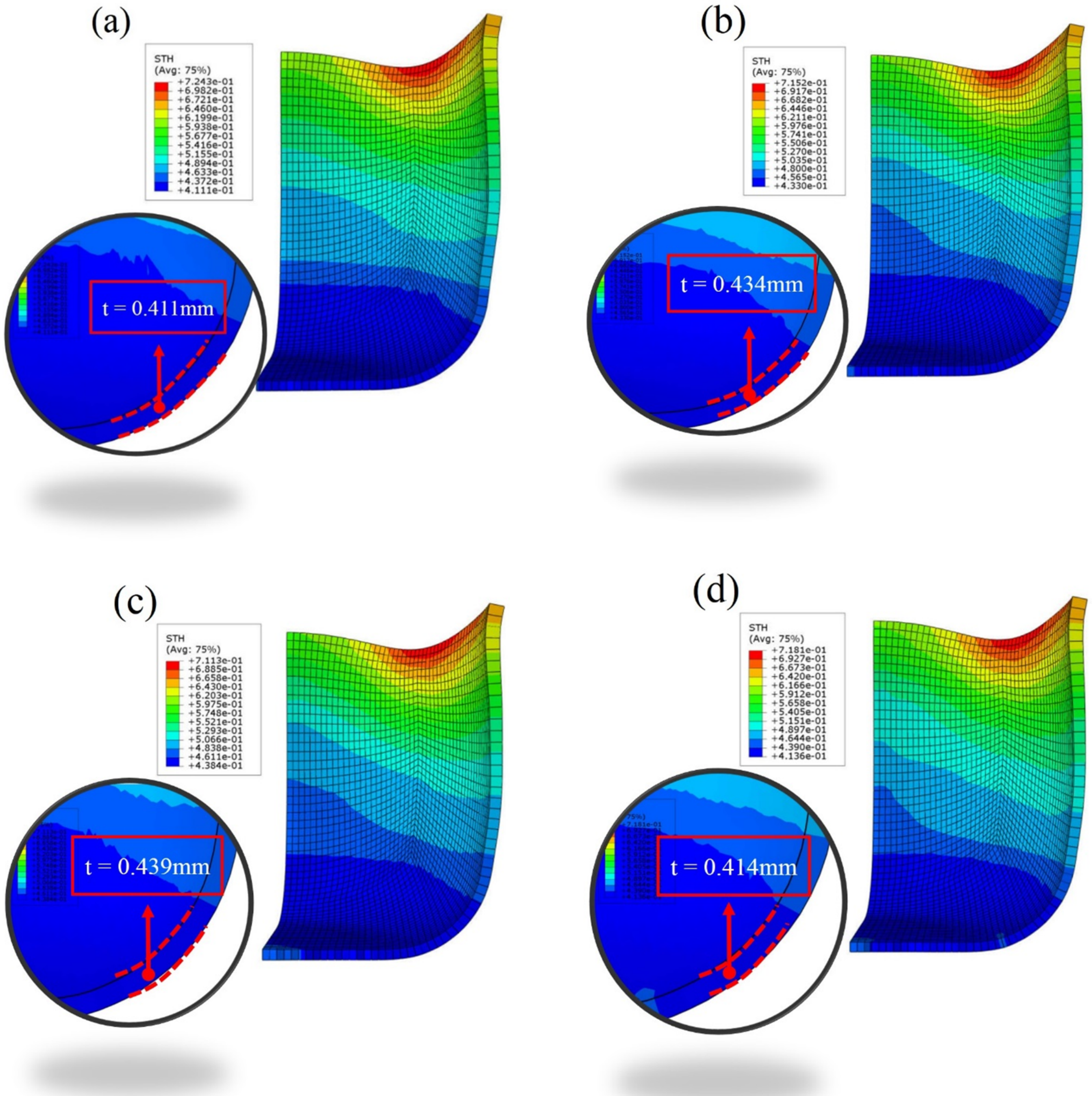

Fig. 12. Effect of vibration frequency on minimum thickness: a) 20kHz, b) 30kHz, c) 35kHz, (d) 40kHz.

Table 5
Input factors and related levels in ultrasonically assisted deep drawing process.

Factors	Symbol	Levels		
		Lowest (−1)	Middle (0)	Highest (+1)
Blank diameter (mm)	BD	34	36.5	39
Punch nose radius (mm)	PNR	2	4	6
Die nose radius (mm)	DNR	2	4	6
Clearance (mm)	Cl	0.55	0.775	1
Amplitude (mμ)	Amp	5	20	35
Frequency (kHz)	Fre	20	40	60

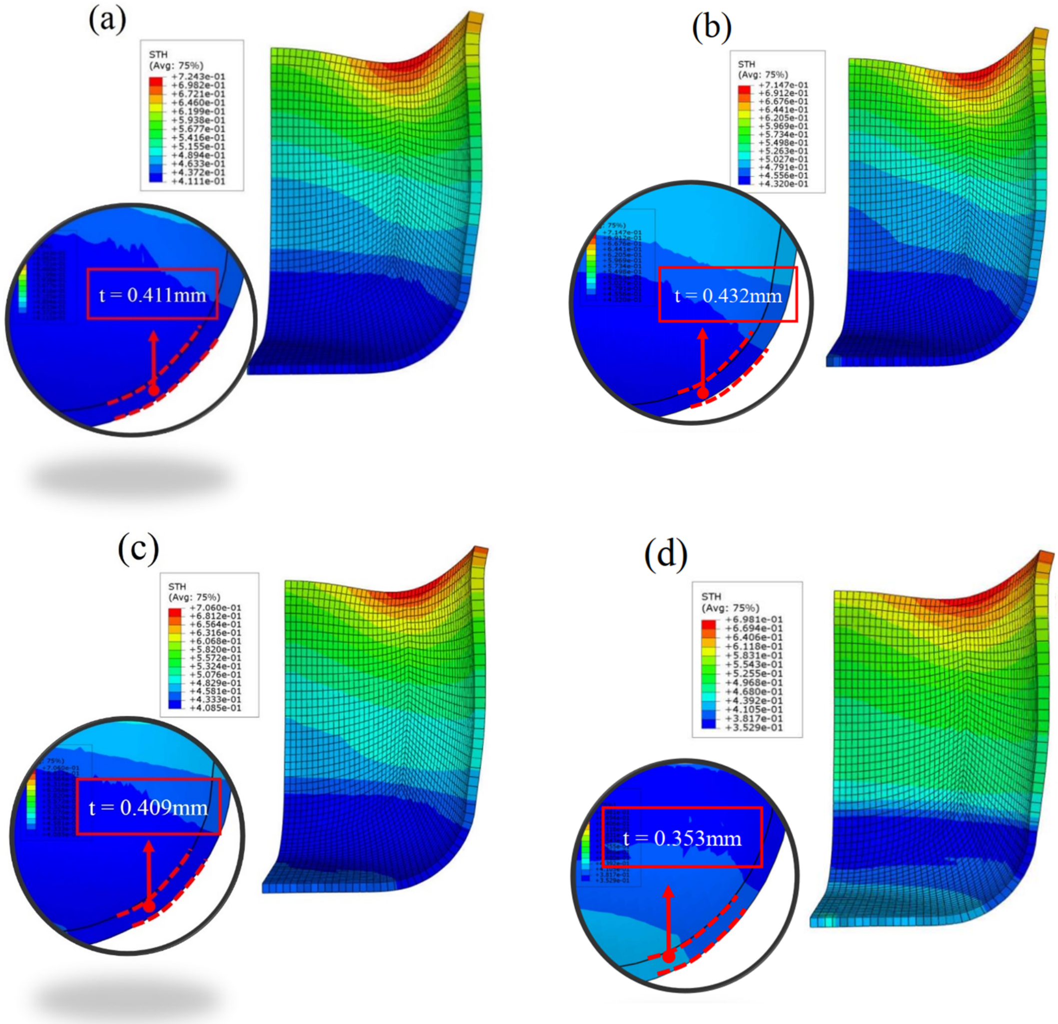

Fig. 13. Effect of vibration amplitude on minimum thickness: a) 5μm, b) 10μm, c) 25μm, d) 35μm.

Table 6
Full factorial design and simulation results in ultrasonically assisted deep drawing process.

	Process parameters						Simulation results	
Run number	BD (mm)	PNR (mm)	DNR (mm)	Cl (mm)	Amp (μm)	Fre (kHz)	Maximum drawing force (N)	Minimum thickness (mm)
1	39	6	2	1	35	60	8555.81	0.361
2	39	6	6	1	5	60	8675.37	0.426
3	36.5	4	4	0.775	20	40	6728.06	0.459
4	36.5	4	6	0.775	20	40	6040.18	0.460
5	34	6	2	0.55	35	60	6818.50	0.389
6	39	6	2	1	5	20	10837.6	0.412
7	39	2	2	1	35	60	6736.95	0.371
8	34	2	2	0.55	35	20	5705.52	0.398
9	36.5	4	4	0.775	20	40	6728.06	0.459
10	36.5	2	4	0.775	20	40	6228.64	0.460
11	36.5	4	4	0.775	20	40	6728.06	0.459
12	34	6	2	1	5	20	9150.58	0.446
13	34	6	6	1	5	20	8153.21	0.468
14	36.5	4	4	0.775	20	40	6728.06	0.459
15	39	6	2	1	5	60	9856.61	0.416
16	36.5	4	4	0.775	20	40	6728.06	0.459

Continuation of the table

	Process parameters						Simulation results	
Run number	BD (mm)	PNR (mm)	DNR (mm)	Cl (mm)	Amp (μm)	Fre (kHz)	Maximum drawing force (N)	Minimum thickness (mm)
17	34	2	6	0.55	5	60	5789.21	0.469
18	39	2	6	0.55	5	60	6856.50	0.433
19	36.5	4	4	0.775	20	40	6728.06	0.459
20	34	6	6	0.55	35	60	5821.13	0.340
21	34	4	4	0.775	20	40	6160.20	0.470
22	34	2	2	1	35	60	6093.77	0.402
23	34	6	6	0.55	35	20	5838.39	0.406
24	36.5	4	4	0.55	20	40	6662.10	0.457
25	36.5	4	4	0.775	20	40	6728.06	0.459
26	36.5	4	2	0.775	20	40	7129.48	0.450
27	34	2	6	1	35	60	5096.40	0.413
28	34	2	6	1	5	20	7022.98	0.468
29	36.5	4	4	0.775	20	40	6728.06	0.459
30	34	6	6	1	5	60	7324.95	0.461
31	39	6	6	1	35	60	7374.57	0.372
32	34	6	2	1	35	60	7224.00	0.392
33	36.5	4	4	0.775	20	20	7023.00	0.457
34	34	6	2	0.55	5	60	7916.81	0.447
35	39	2	2	1	5	20	9498.96	0.422
36	36.5	4	4	0.775	20	40	6728.06	0.459
37	39	6	2	0.55	35	20	8095.99	0.412
38	36.5	4	4	0.775	20	60	7320.77	0.441
39	39	6	6	1	35	20	7395.01	0.377
40	34	2	6	0.55	5	20	6617.47	0.465
41	39	2	6	1	5	20	8317.72	0.432
42	34	2	2	0.55	5	60	6786.58	0.458
43	34	6	6	0.55	5	20	7747.71	0.454
44	34	2	6	0.55	35	60	4690.90	0.410
45	34	2	2	0.55	5	20	7614.84	0.454
46	39	6	6	0.55	35	60	6894.31	0.369
47	39	6	6	0.55	5	60	8164.45	0.423
48	34	2	2	1	5	20	8020.34	0.457
49	39	6	2	0.55	35	60	8075.55	0.359
50	39	6	6	1	5	20	9656.33	0.422
51	34	6	2	0.55	5	20	8745.07	0.443
52	36.5	6	4	0.775	20	40	7463.06	0.450
53	39	2	2	1	35	20	7237.65	0.377
54	34	6	2	1	35	20	7241.26	0.398
55	34	6	2	1	5	60	8322.32	0.450
56	39	2	6	0.55	5	20	7837.46	0.429
57	39	2	6	1	35	20	6056.41	0.387
58	34	6	6	1	35	60	6226.64	0.403
59	34	2	2	1	35	20	6111.03	0.409
60	34	2	6	0.55	35	20	4708.16	0.417
61	39	2	6	1	5	60	7336.76	0.436
62	39	6	2	0.55	5	60	9376.34	0.413
63	36.5	4	4	0.775	20	40	6728.06	0.459
64	39	4	4	0.775	20	40	7295.89	0.440
65	36.5	4	4	0.775	20	40	6728.06	0.459
66	36.5	4	4	0.775	20	40	6728.06	0.459
67	39	2	2	1	5	60	8518.00	0.425
68	39	2	6	1	35	60	6035.97	0.382

Continuation of the table

	Process parameters						Simulation results	
Run number	BD (mm)	PNR (mm)	DNR (mm)	Cl (mm)	Amp (μm)	Fre (kHz)	Maximum drawing force (N)	Minimum thickness (mm)
69	39	6	6	0.55	5	20	9176.06	0.419
70	39	2	2	0.55	35	60	6736.95	0.369
71	34	6	6	1	35	20	6243.89	0.409
72	36.5	4	4	0.775	35	40	6002.49	0.407
73	34	6	6	0.55	5	60	6919.45	0.458
74	34	2	2	1	5	60	7192.08	0.461
75	34	2	6	1	5	60	6194.72	0.472
76	34	6	2	0.55	35	20	6835.76	0.395
77	39	2	2	0.55	5	20	9018.70	0.419
78	34	2	2	0.55	35	60	5688.27	0.399
79	39	2	2	0.55	5	60	8037.74	0.423
80	36.5	4	4	0.775	5	40	7227.48	0.468
81	36.5	4	4	0.775	20	40	6728.06	0.459
82	39	2	2	0.55	35	20	6757.38	0.374
83	36.5	4	4	0.775	20	40	6728.06	0.459
84	36.5	4	4	1	20	40	7104.98	0.460
85	39	6	6	0.55	35	20	6914.75	0.375
86	39	2	6	0.55	35	20	5576.15	0.385
87	39	6	2	0.55	5	20	10357.3	0.426
88	34	2	6	1	35	20	5113.66	0.420
89	39	2	6	0.55	35	60	4690.90	0.379
90	39	6	2	1	35	20	8576.25	0.367

Based on a sequence of designed experiments, this methodology optimizes the process to choose the most appropriate condition by establishing a logical link between the inputs and outputs. One of the most popular methods of DOE is the Central Composite Design (CDD) using full factorial type. This method investigates all feasible cases of factors at different levels. In this paper, the layout of the run for simulations was performed based on a central composite-full factorial design approach. The process predominant parameters of UADD and its levels that utilized in the numerical study are provided in Table 5. Pursuant to full factorial design considering six independent factors at three different values, number of 90 simulations were determined and performed. Table 6 presents the full factorial design of the process parameters along with maximum average drawing force and minimum thickness of the formed cup achieved from simulation results in UADD operation.

3.4. Development Mathematical Model

Design Expert (version 10) package as a commercial statistical software was employed to establish mathematical relationship between process parameters and simulation results by RSM and through analysis of second order full quadratic regression model. The general form of this mathematical model is shown in Eq. (19) [6].

$$y = b_0 + \sum_{i=1}^{n} b_i X_{iu} + \sum_{i=1}^{n} b_{ii} X_{iu}^2 + \sum_{i=1}^{n} X_{iu} X_{ju} \quad (20)$$

where y is the response function, b_0, b_i, b_{ii}, b_{ij} are constant coefficients, n is the number of factors; x_{iu}^2 is the second-order variable term; $x_{iu}x_{ju}$ are the interaction terms. It is worth mentioning that non-significant terms of developed mathematical model may be omitted for analysis without adverse effect. Therefore, an analysis of variance (ANOVA) procedure considering coefficient of determination i.e. R^2 was performed to assess the significant terms of the regression model. Tables 7 and 8 represent ANOVA results of maximum forming force and minimum thickness, respectively. In the deep drawing process, as the punch penetrates the die cavity, the forming force increases continuously and reaches a peak value, then as the punch continues to move for the final forming of the cup, the amount of force also decreases. Therefore, due to the friction conditions between the sheet and the tool surfaces, it is possible that the sheet in the position of peak force leads to severe thinning and rupture. Reducing the maximum average forming force can prevent the sheet from rupturing and the part can be fully formed. Therefore, the specific value of the maximum force and its reduction due to changing process parameters was investigated in this study. The most effective parameters on the specified responses and the efficiency of developed mathematical models can be found using the data in this table. It is seen from Tables 7 and 8 that for both the forming force and minimum thickness the F-Value for the models are 303.80 and 128.87, respectively. These values imply the model terms are significant. It is worth noting that the clearance parameter does not have a significant effect on the minimum thickness. The presence of ultrasonic vibration in the deep drawing process leads to a micro-gap between the sheet and the working surface of the die. On the other hand, the friction of the inner wall of the die and the formed cup also is reduced. Hence, vibration amplitude plays a pivotal role in reducing friction and clearance changes do not dominate its effects. The vibration amplitude, in addition to facilitating the material flow into the die cavity, has a significant effect on reducing friction in the cup formatting stage and leads to improved thickness distribution. Mathematical relations are provided for both forming force and minimum thickness outputs in Eqs. (20) and (21).

$$\begin{aligned}&\text{Forming force (N)} = 6716.51 + 596 \times A\\&+ 637.12 \times B - 550.94 \times C + 227.73 \times D\\&- 834.81 \times E - 240.20 \times F + 72.63 \times AB\\&- 52.46 \times AC - 89.85 \times AE - 40.98 \times AF\\&+ 200.90 \times EF + 155.63 \times D^2 + 443.97 \times F^2 \qquad (21)\end{aligned}$$

$$\begin{aligned}&\text{Minimum thickness (mm)} = +0.46 - 0.016 \times A\\&- 3.884E - 3 \times B + 4.608E - 3 \times C - 0.026 \times E\\&- 1.785E - 3 \times F - 1.504E - 3 \times AC + 1.796E\\&- 3 \times AE - 2.664E - 3 \times EF - 0.029 \times E^2\\&- 0.014 \times F^2 \qquad (22)\end{aligned}$$

Table 7
ANOVA results of maximum average forming force in UADD process.

Source	Sum of square	Degree of freedom	Mean of squares	F-value	P-value Prob>F	Contribution (%)	Significant
Model	1.33E+08	13	1.33E+08	629.879	< 0.0001		*
A-BD	2.35E+07	1	2.35E+07	1443.91	< 0.0001	19.03	*
B-PNR	2.68E+07	1	2.68E+07	1645.31	< 0.0001	21.68	*
C-DNR	2.00E+07	1	2.00E+07	1230.3	< 0.0001	16.21	*
D-CL	3.42E+06	1	3.42E+06	210.21	< 0.0001	2.77	*
E-Amp	4.60E+07	1	4.60E+07	2824.7	< 0.0001	37.22	*
F-Fre	3.81E+06	1	3.81E+06	233.86	< 0.0001	3.09	*
AB	3.38E+05	1	3.38E+05	20.73	< 0.0001		*
AC	1.76E+05	1	1.76E+05	10.81	0.0015		*
AE	5.17E+05	1	5.17E+05	31.73	< 0.0001		*
AF	1.08E+05	1	1.08E+05	6.6	0.0122		*
EF	2.58E+06	1	2.58E+06	158.64	< 0.0001		*
D^2	91376.07	1	91376.07	5.61	0.0204		*
F^2	7.44E+05	1	7.44E+05	45.67	< 0.0001		*
$R^2 = 0.9908$, $R^2_{adj} = 0.9892$ and $R^2_{pred} = 0.9858$							
Adequacy precision is 122.767							

Table 8
ANOVA results of minimum thickness in UADD process.

Source	Sum of square	Degree of freedom	Mean of squares	F-value	P-value Prob>F	Contribution (%)	Significant
Model	0.093	10	9.32E-03	290.99	< 0.0001		*
A-BD	0.016	1	0.016	499.22	< 0.0001	25.86	*
B-PNR	9.96E-04	1	9.96E-04	31.1	< 0.0001	1.61	*
C-DNR	1.40E-03	1	1.40E-03	43.77	< 0.0001	2.27	*
E-Amp	0.043	1	0.043	1350	< 0.0001	69.92	*
F-Fre	2.10E-04	1	2.10E-04	6.57	0.0123	0.34	*
AC	1.45E-04	1	1.45E-04	4.52	0.0366		*
AE	2.06E-04	1	2.06E-04	6.45	0.0131		*
EF	4.54E-04	1	4.54E-04	14.19	0.0003		*
E^2	3.08E-03	1	3.08E-03	96.11	< 0.0001		*
F^2	7.60E-04	1	7.60E-04	23.74	< 0.0001		*
$R^2 = 0.9736$, $R^2_{adj} = 0.9702$ and $R^2_{pred} = 0.9634$							
Adequacy precision is 55.156							

3.5. Parametric Influence

3.5.1. Forming Force

Fig. 14 shows the effect of process factors on the forming force of the ultrasonic-assisted deep drawing process. As can be seen in Fig. 14a, increasing the initial blank diameter increases the forming force. This can be mainly due to the increase in the initial blank diameter which leads to increase in the friction of the sheet and die's surface. Besides, the larger blank diameter increases the contact of sheet surface and the blank holder, and as a result, the blank material flow into the die cavity becomes more difficult and the forming process becomes harder. Fig. 14b shows the effect of the punch edge radius variation on the forming force. As can be seen in this plot, an increase in the punch edge radius increases the force. Larger radius reduces the contact of punch and the sheet and makes the shaping process more difficult and increases the required force. Fig. 14c demonstrates the effect of the die edge radius on the forming force. It is quite clear that by increasing the die edge radius, the forming force decreases. By increase in the die edge radius, the blank flows in a smaller path and finally the required force sheet bending is less. Fig. 14d displays the effect of clearance on the forming force. Based on the ANOVA analysis, this parameter has an insignificant effect on the forming force comparing to the other factors. However, choosing the right amount of clearance can partially reduce the forming force. It can be seen that an increase in the amount of clearance increases the forming force. Fig. 14e illustrates the effect of the vibration amplitude on the forming force. The result of ANOVA (Table 7) shows that the amplitude of ultrasonic vibration is the most significant parameter. A continuous increase in the ultrasonic vibration amplitude decreases the forming force. The main reason is the existence of a continuous micro-gap between the working surface of the die and the blank in the ultrasonic vibration mechanism. Hence, as the vibration amplitude increases, the created gap increases and reduces the friction. Finally, the blank material flow into the die cavity becomes easier. Fig. 14f shows the effect of another ultrasonic vibration parameter, the vibration frequency. As shown in the figure, there is an optimal value for the UV frequency, and increasing the vibration frequency up to about 50kHz leads to a decrease in the forming force. By further increasing the frequency, the forming force increases. The very first reason behind this phenomenon is that increasing the frequency of vibrations causes shorter period for the die to come to initial state and be separated from the sheet (micro-gap state). On the other hand, a rebound occurs at the moment of separation between the surface of the work-piece flange and the working surface of the die.

3.5.2. Thickness Reduction

Fig. 15 depicts the effect of UADD process parameters on the minimum thickness. As shown in Fig. 15a, when the blank diameter increases, thinning in the formed cup increases. This is because an increase in the blank diameter leads to increase the drawing ratio. Fig. 15b illustrates the effect of the punch edge radius on the thickness reduction. According to this figure, the increase in the punch edge radius reduces the thinning of the sheet. Thinning often occurs at the circumference position of the punch head. As discussed earlier, an increase in the punch edge results in the overall surface of the punch head to be less exposed to the sheet. Hence, the nose radius of the cup bottom, which is formatted by the punch edge, is subjected to high tensile stress and increases the thinning in this area of the formed cup. The effect of the die edge radius on the minimum thickness is shown in Fig. 15c. As the die edge radius increases, the flow of the blank material follows a less bent path to enter the die cavity. Hence, increasing this value leads to a decrease in the thinning of the formed cups. Based on the results of ANOVA analysis (Table 8), it was shown that the clearance between the punch and the die has a negligible effect on the work-piece thickness. To have a better understanding, Fig. 15d shows the amount of minimum thickness. The decrease in clearance also has a negligible effect on the increase in the minimum thickness. By decreasing the clearance, the ironing effect on the walls leads to a slight decrease in the thickness of the cup. According to the ANOVA analysis, one of the most important parameters of the ultrasonic assisted deep drawing process is the vibration amplitude (Table 8). The simulation results, Fig. 15e, show that by increasing the vibration amplitude up to 11μm, the workpiece has a better thickness distribution. However, increasing the vibration amplitude leads to an increase in the thinning. The main reason can be the micro-hammer behavior on the surface of the blank's flange in high amplitude. Applying high amplitude ultrasonic vibrations can reduce the forming force, but this will not be very useful for the thickness distribution at the end. Incorrect selection of the ultrasonic vibration amplitude in the sheet forming processes leads to higher thinning values, which is a disadvantage. Fig. 15f shows the effect of the frequency on the maximum thickness reduction of the work-piece. It is also clear that an increase in the ultrasonic vibration frequency up to the optimum value decreases the thinning. In higher frequencies than optimum, the thickness reduction trend is reversed and the thinning is more significant. The main cause of this phenomenon, as explained in the previous section, is the reduction of the work-piece and die separation period.

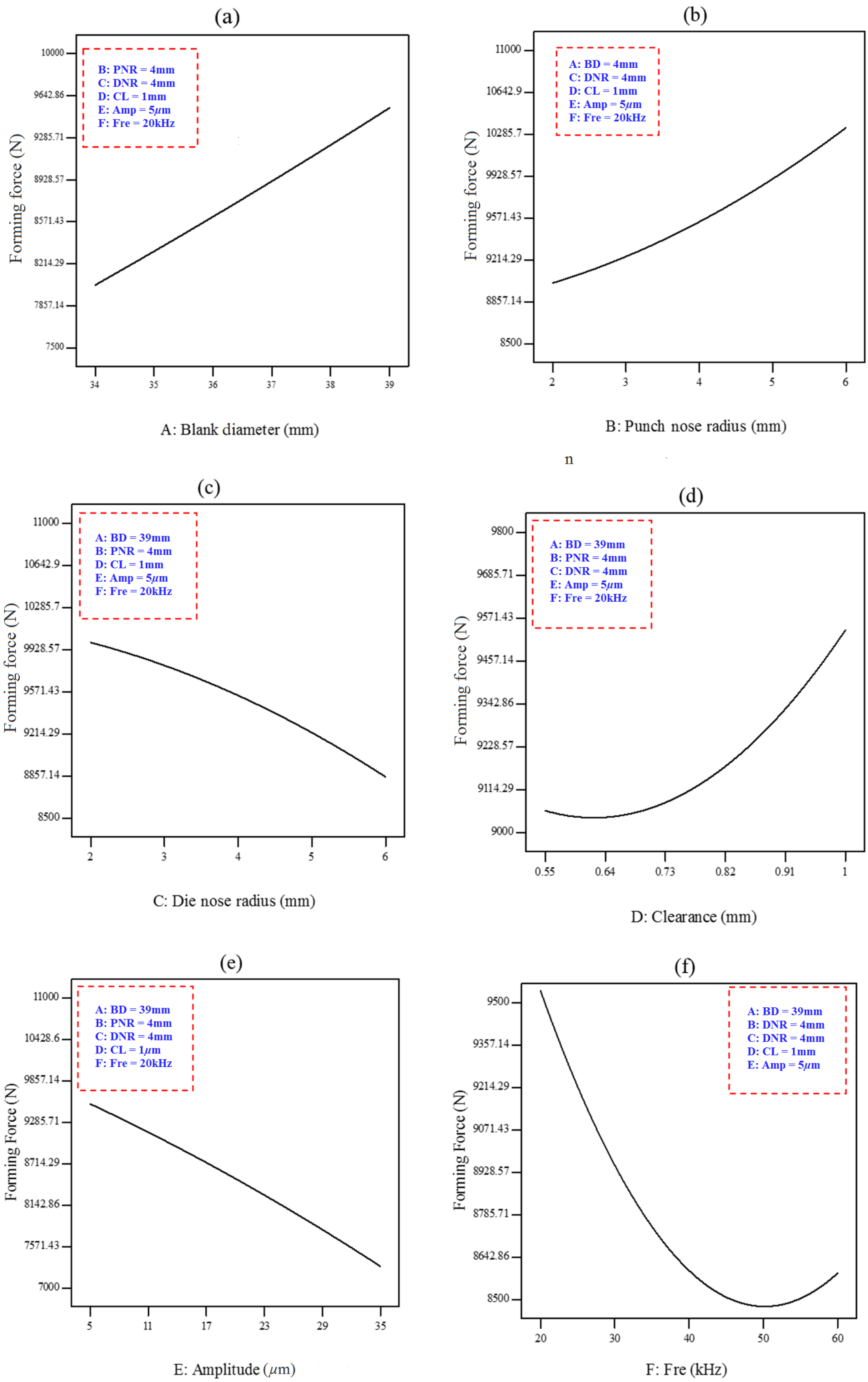

Fig. 14. The effect of process independent parameters on the required forming force.

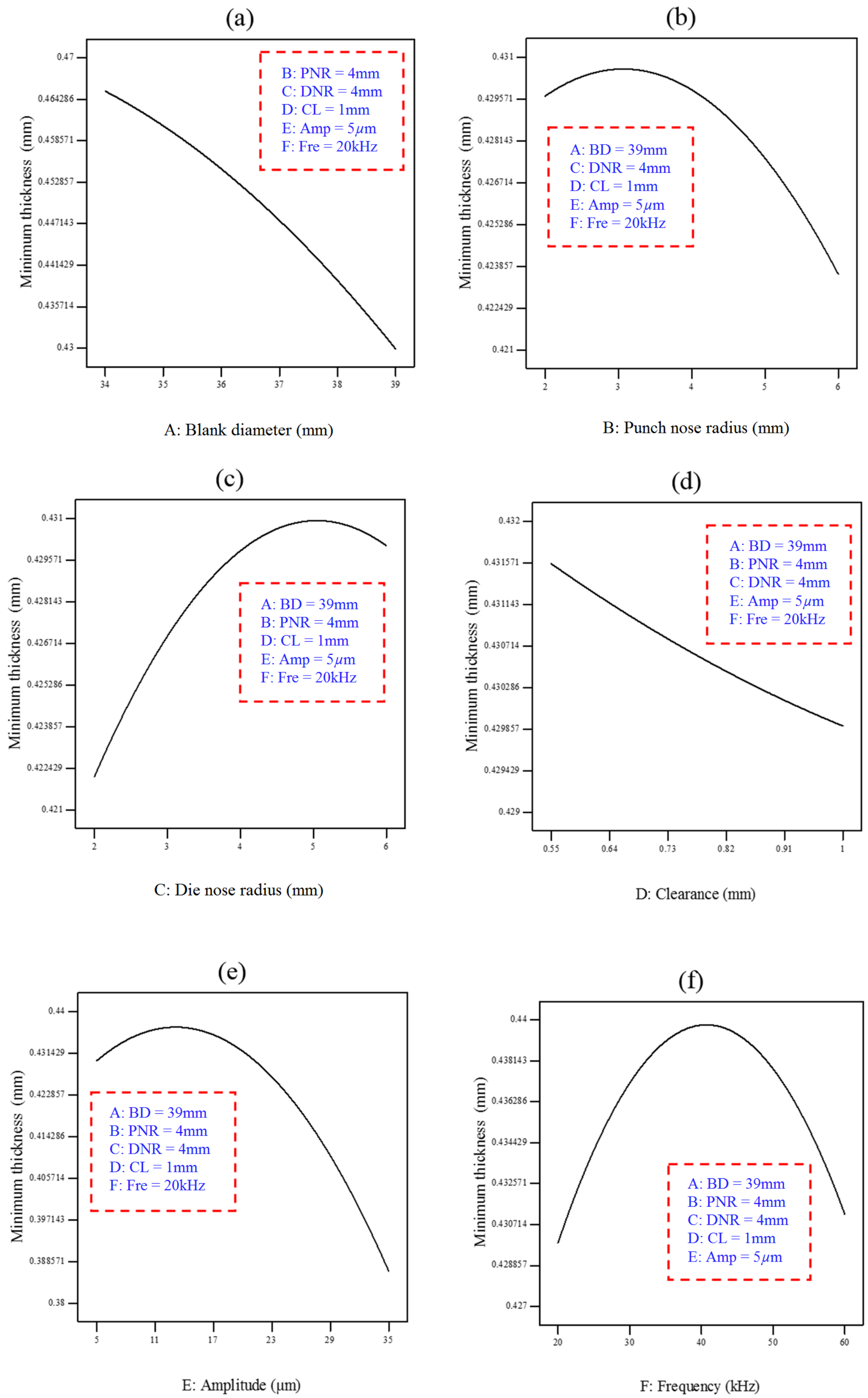

Fig. 15. Effect of process parameters on the minimum thickness of the formed part.

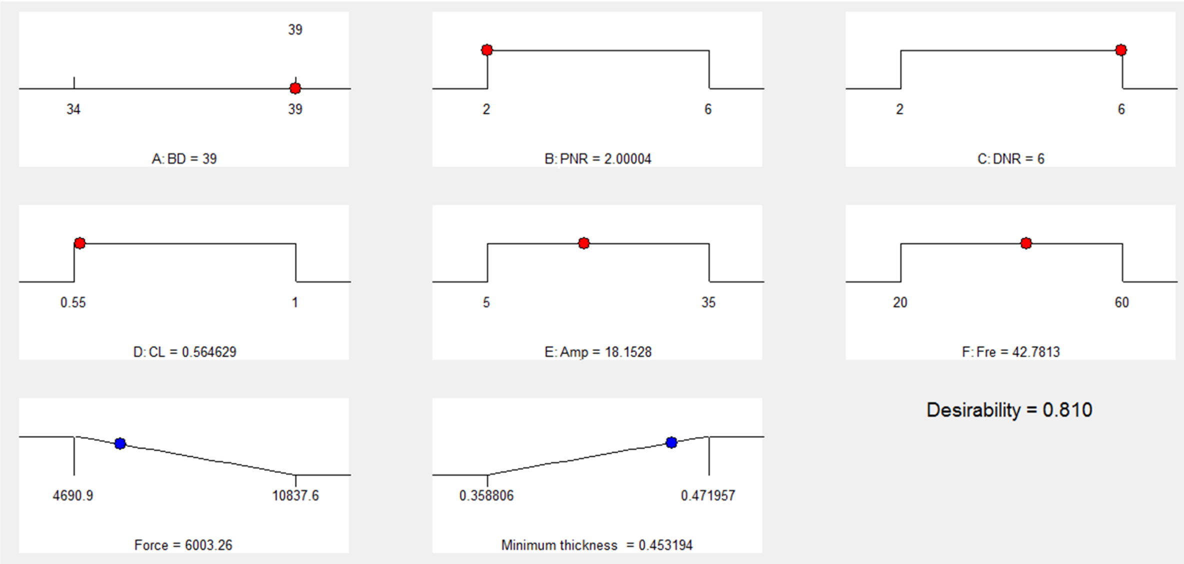

Fig. 16. Final results of optimized parameters in UADD process.

3.5.3. Optimization

Optimization of process was done by RSM method. The minimum amount of the peak of the forming force and the maximum amount of thickness was defined as the optimization criteria. Furthermore, the highest value was given for the diameter of initial blank. Because, the goal of deep drawing process is to achieve cups with higher height. On the other hand, the rest of the parameters were considered in the predetermined range. As shown in Fig. 16, the optimal values for the two important parameters of frequency and amplitude of ultrasonic vibrations were obtained 42.8kHz and 18μm, respectively.

4. Conclusions

In this study, a customized ultrasonic-die with axial vibration capability was designed and manufactured to perform a series of deep drawing experimental tests, considering both conventional and ultrasonic assisted condition. The finite element model was subsequently developed to simulate the deep drawing process. In order to provide a logical relationship between the input and output parameters of the forming process (including the forming force and minimum thickness of the formed cup), a central composite test design method was used. In this way, 90 simulations with a different combination of parameters were proposed. Then, to estimate the forming force and the amount of thickness reduction under different conditions, high-reliability regression models were developed. The main conclusions drawn are the following:

1. Results of experimental test show a 6% decrease in the vibration conditions (20kHz frequency and 5μm amplitude) and a 12% increase in the drawing ratio when compared to the conventional deep drawing.

2. Based on the Response Surface Method (RSM) experiment design, several number of models with different parameters were simulated. The regression models were presented to estimate the forming force and minimum thickness of the formed cups. The regression equations for these two output parameters provide promising results.

3. The results of the ANOVA for the forming force indicates that the vibration amplitude and initial blank diameter are the two most important factors. Moreover, an increase in vibration amplitude up to 35μm generates a micro-impacts regime, which significantly reduces the forming force. On the other hand, due to the rebound phenomenon, an increase in the UV frequency leads to an insignificant reduction in forming force.

4. The obtained output parameter of the minimum work-piece thickness from ANOVA showed that the vibration amplitude had a significant impact to the thickness value. The high-amplitude impacts cause a significant plastic strain and thinning in the work-piece, which has a major drawback to sheet metal forming processes such as deep drawing.

5. Optimization of process was performed by RSM method. The optimal values for the two important parameters of frequency and amplitude of ultrasonic vibrations were obtained 42.8kHz and 18μm, respectively.

References

[1] W.D. Li, B. Meng, C. Wang, M. Wan, L. Xu, Effect of pre-forming and pressure path on deformation behavior in multi-pass hydrodynamic deep drawing process, Int. J. Mech. Sci., 121 (2017) 171-180.

[2] E. Afshin, M. Kadkhodayan, An experimental investigation into the warm deep-drawing process on laminated sheets under various grain sizes, Mater. Des., 87 (2015) 25-35.

[3] S. Fan, J. Mo, J. Fang, J. Xie, Electromagnetic pulse-assisted incremental drawing forming of aluminum alloy cylindrical part and its control strategy, Int. J. Adv. Manuf. Technol., 95 (2018) 2681-2690.

[4] I. Irthiea, Experimental and numerical evaluation of micro flexible deep drawing technique using floating ring, J. Manuf. Process., 38 (2019) 556-563.

[5] A. Mostafapur, S. Ahangar, R. Dadkhah, Numerical and experimental investigation of pulsating blankholder effect on drawing of cylindrical part of aluminum alloy in deep drawing process, Int. J. Adv. Manuf. Technol., 69 (2013) 1113-1121.

[6] B.T. Lin, C.Y. Yang, Applying the Taguchi method to determine the influences of a microridge punch design on the deep drawing, Int. J. Adv. Manuf. Technol., 88 (2017) 2109-2119.

[7] J. Hu, T. Shimizu, T. Yoshino, T. Shiratori, M. Yang, Evolution of acoustic softening effect on ultrasonic-assisted micro/meso-compression behavior and microstructure, Ultrasonics, 107 (2020) 106107.

[8] V. Fartashvand, A. Abdullah, S.A. Sadough Vanini, Investigation of Ti-6Al-4V alloy acoustic softening, Ultrason. Sonochem., 38 (2017) 744-749.

[9] F. Blaha, B. Langenecker, Tensile deformation of zinc crystal under ultrasonic vibration, Naturwissenschaften, 42(556) (1955) 1-10.

[10] M.A. Rasoli, A. Abdullah, M. Farzin, A. Fadaei Tehrani, A. Taherizadeh, Influence of ultrasonic vibrations on tube spinning process, J. Mater. Process. Technol., 212(6) (2012) 1443-1452.

[11] S. Dong, M.J. Dapino, Elastic-plastic cube model for ultrasonic friction reduction via Poisson's effect, Ultrasonics, 54 (2014) 343-350.

[12] J. Hu, T. Shimizu, M. Yang, Investigation on ultrasonic volume effects: Stress superposition, acoustic softening and dynamic impact, Ultrason. Sonochem., 48 (2018) 240-248.

[13] F. Djavanroodi, H. Ahmadian, K. Koohkan, R. Naseri, Ultrasonic assisted-ECAP, Ultrasonics, 53 (2013) 1089-1096.

[14] Y. Liu, Q. Han, L. Hua, C. Xu, Numerical and experimental investigation of upsetting with ultrasonic vibration of pure copper cone tip, Ultrasonics, 53(3) (2013) 803-807.

[15] M. Vahdati, R. Mahdavinejad, S. Amini, Investigation of the ultrasonic vibration effect in incremental sheet metal forming process, Proc. Inst. Mech. Eng. Part B. J. Eng. Manuf., 231(6) (2015) 971-982.

[16] S. Amini, A. Hosseinpour Gollo, H. Paktinat, An investigation of conventional and ultrasonic-assisted incremental forming of annealed AA1050 sheet, Int. J. Adv. Manuf. Technol., 90 (2017) 1569-1578.

[17] Y. Long, Y. Li, J. Sun, I. Ille, J. Li, J. Twiefel, Effects of process parameters on force reduction and temperature variation during ultrasonic assisted incremental sheet forming process, Int. J. Adv. Manuf. Technol., 97 (2018) 13-24.

[18] P. Li, J. He, Q. Liu, M. Yang, Q. Wang, Q. Yuan, Y. Li, Evaluation of forming forces in ultrasonic incremental sheet metal forming, Aerosp. Sci. Technol., 63 (2017) 132-139.

[19] A. Pasierb, A. Wojnar, An experimental investigation of deep drawing and drawing processes of thin - walled products with utilization of ultrasonic vibrations, J. Mater. Process. Technol., 34 (1992) 489-494.

[20] T. Jimma, Y. Kasuga, N. Iwaki, O. Miyazawa, E. Mori, K. Ito, H. Hatano, An application of ultrasonic vibration to the deep drawing process, J. Mater. Process. Technol., 80-81 (1998) 406-412.

[21] M.A. Rasoli, A. Abdullah, M. Farzin, A. Fadaei Tehrani, A. Taherizadeh, Influence of ultrasonic vibrations on tube spinning process, J. Mater. Process. Technol., 212(6) (2012) 1443-1452.

[22] Y. Ashida, H. Aoyama, Press forming using ultrasonic vibration, J. Mater. Process. Technol., 187-188 (2007) 118-122.

[23] E. Malekipour, H. Heidary, N. Shahbazi Majd, S. Mazdak, E. Sharifi, Effect of resonant frequency variation on the ultrasonically assisted deep drawing process: numerical and experimental study, Int. J. Adv. Manuf. Technol., 106 (2020) 2243-2264.

[24] R. Hill, A theory of the yielding and plastic flow of anisotropic metals, Proc. R. Soc. London. Ser. A Math. Phys. Sci., 193 (1948) 281-297.

[25] Q. Mao, N. Coutris, H. Rack, G. Fadel, J, Gibert, Investigating ultrasound-induced acoustic softening in aluminum and its alloys, Ultrasonics, 102 (2020) 106005.

[26] V.C. Kumar, I.M. Hutchings, Reduction of the sliding friction of metals by the application of longitudinal or transverse ultrasonic vibration, Tribol. Int., 37 (2004) 833-840.

[27] Z. Sheng, S. Jirathearanat, T. Altan, Adaptive FEM simulation for prediction of variable blank holder force in conical cup drawing, Int. J. Mach. Tools. Manuf., 44 (2004) 487-494.